Polymer Chemistry

Accepted Manuscript

This is an *Accepted Manuscript*, which has been through the Royal Society of Chemistry peer review process and has been accepted for publication.

Accepted Manuscripts are published online shortly after acceptance, before technical editing, formatting and proof reading. Using this free service, authors can make their results available to the community, in citable form, before we publish the edited article. We will replace this *Accepted Manuscript* with the edited and formatted *Advance Article* as soon as it is available.

You can find more information about *Accepted Manuscripts* in the Information for Authors.

Please note that technical editing may introduce minor changes to the text and/or graphics, which may alter content. The journal's standard Terms & Conditions and the Ethical guidelines still apply. In no event shall the Royal Society of Chemistry be held responsible for any errors or omissions in this *Accepted Manuscript* or any consequences arising from the use of any information it contains.

ROYAL SOCIETY OF CHEMISTRY

www.rsc.org/polymers

Low band-gap copolymers derived from fluorinated isoindigo and dithienosilole: synthesis, properties and photovoltaic applications

Zhenguo Wang,[a] Jie Zhao,[ab] Ying Li,[a] and Qiang Peng[a*]

[a] Key Laboratory of Green Chemistry and Technology of Ministry of Education, College of Chemistry, Sichuan University, Chengdu 610064, P. R. China

[b]School of Environmental and Chemical Engineering, Nanchang Hangkong University, Nanchang 330063, P. R. China

*To whom correspondence should be addressed: Tel: +86-28-86510868; fax: +86-28-86510868; e-mail: qiangpengjohnny@yahoo.com

Polymer Chemistry Accepted Manuscript

Abstract:

A low band-gap copolymer **PDTS-FID** alternating dithienosilole (**DTS**) donor block with fluorinated isoindigo (**FID**) unit and its non-fluorinated counterpart **PDTS-ID** have been synthesized and characterized for photovoltaic applications. Compared to **PDTS-ID**, the isoindigo fluorination enables **PDTS-FID** to process broader and stronger absorption, lower-lying HOMO and LUMO energy levels, and higher hole mobility, resulting in improved open-circuit voltage (V_{oc}), short-circuit current density (J_{sc}), fill factor (FF) as well as power conversion efficiency (PCE). The positive effect was attributed to the fluorinated isoindigo block favored linear and planar conformation, giving rise to better backbone packing of the related copolymer, which was also confirmed by theoretical calculations (DFT). The conventional and inverted devices were fabricated and evaluated to explore the photovoltaic properties of the resulting copolymers. The best performance of 5.79% PCE was obtained from an inverted polymer solar cell (PSC) using **PDTS-FID** as the donor material, with a V_{oc} of 0.84 V, J_{sc} of 10.77 mA cm^{-2} and FF of 0.64. These low band-gap copolymers could be expected as the promising donor materials in application of PSCs.

Keywords: Polymer solar cell, fluorination, isoindigo, dithienosilole, planar conformation

Polymer Chemistry Accepted Manuscript

Introduction

Polymer solar cells (PSCs) have attracted wide attention due to their unique advantages, such as low cost, light weight, flexibility and large-area manufacturing compatibility.[1] To achieve more better performance for commercialization of PSCs, the rational molecular design and effective preparation of polymeric donor materials is one of the hot and important topics. To enhance the absorption and improve carrier mobility, low band-gap (LBG) conjugated polymers were developed by incorporating electron-rich donor (D) and electron-deficient acceptor (A) segments into the polymer backbones.[2,3] This push-pull interaction of the donor and acceptor moieties can efficiently induce a lower-energy absorption band and control the energy levels (HOMO and LUMO) due to the intramolecular charge transfer (ICT) processes and hybridization of their molecular orbitals.[4] Based on this strategy, the power conversion efficiency (PCE) of over 7% were obtained by using LBG conjugated copolymers as donor materials in bulk-heterojunction (BHJ) solar cells.[5,6]

Isoindigo (ID) was an efficient acceptor block for its strong electron-withdrawing character and large optical transition dipole with two lactam rings, which could be utilized for constructing LBG copolymers. The application of isoindigo in organic solar cells was first introduced by the Reynolds *et al.* in 2010, the reported isoindigo-based oligomer, exhibited a PCE of 1.76%.[7] Later, the same group designed and synthesized a series of isoindigo-based copolymers with broad absorption spectrum, low-lying LUMO and HOMO energy levels, but their photovoltaic performance was not investigated.[8] Almost at the same time, Zhang et al. and Zou *et*

Polymer Chemistry Accepted Manuscript

al. reported some isoindigo-based D-A copolymers with different donor blocks with PCEs ranging from 0.02 to 1.91%.[9,10] Using thiophene as a donor block with designed side chains, Andersson *et al.* reported a new isoindigo-based copolymer, **PTI-1**, which showed a PCE up to 3.0%.[11] Shortly after that, the same group synthesized another isoindigo-based copolymer with terthiophene as a donor block affording 6.3% PCE.[12] Some other types of donor blocks, such as dithienosilole, benzodithiophene, cyclopentadithiophene, 9-alkylidene-9H-fuorene, naphthalene and anthracene, were also copolymerized with isoindigo, and the resulting copolymers processed good photovoltaic performance in PSCs.[13]

It is interesting to note that the isoindigo-based copolymers reported so far own low-lying HOMO (-5.50～-5.90 V) and LUMO (-3.70～-4.00 V) energy levels. These copolymers also exhibit promising broad absorption even towards the near-IR region by choosing appropriate conjugated donors with variable low bandgaps ranging from 1.3 to 1.8 eV. How to extend the photovoltaic application of isoindigo and modified isoindigo has been emerged as a challenge for achieving high efficiency over 10% in the near future. In 2012, Pei *et al.* designed a fluorinated isoindigo unit (**FID**) and synthesized a newly isoindigo-based copolymer (**PFII2T**) with lowered bandgaps, HOMO and LUMO energy levels. High-performance ambipolar field-effect transistors (FETs) with good ambient stability were obtained by using PFII2T as the active material. The electron mobility increases from 10^{-2} to 0.43 $cm^2\ V^{-1}\ s^{-1}$ with high hole mobility up to 1.85 $cm^2\ V^{-1}\ s^{-1}$.[14] Very recently, we used bis(dialkylthienyl) benzodithiophene (**BDTT**) and fluorinated isoindigo unit (**FID**) as the donor and

Polymer Chemistry Accepted Manuscript

accepter, respectively, and prepared a new LBG conjugated copolymer (**PBDTT–FID**), which exhibited exciting solar cell performance with 7.04% PCE value.[15] Motivated by the merits of low-lying energy levels, extended light absorption as well as high hole mobility afforded by **FID** units, it is well worth studying the photovoltaic properties of other **FID**-based copolymers with different donor blocks. In this paper, we would reported in detail the synthesis, characterization and solar cell properties of a new LBG copolymer containing alternated dithieno[3,2-b:2',3'-d]silole (**DTS**) and **FID** blocks. For deeper analysis of the fluorination effect, the copolymer with **DTS** and **ID** was also synthesized and investigated.

Results and discussion

Synthesis and characterization

The synthetic route to the designed copolymers is showed in **Scheme 1**. 6,6'-Bis(5-bromothiophen-2-yl)-N,N'-(2-ethylhexyl)isoindigo (**ID**),[15] 6,6'-bis(5-bromothiophen-2-yl)-7,7'-difluoro-N,N'-(2-ethylhexyl)isoindigo (**FID**)[14,15] and 4,4'-dioctyl-5,5'-bis(tributyltin)-dithieno[3,2-b:2',3'-d]silole (**DTS-Sn**),[16] were synthesized according to the literature methods. Polymers **PDTS-ID** and **PDTS-FID** were prepared through Stille-coupling polymerization between the bromide isoindigo (**ID** or **FID**) and the organic tin monomers (**DTS-Sn**) under argon protection, using $Pd_2(dba)_3$ as catalyst and P(*o*-tolyl)$_3$ as ligand. The crude copolymers were treated by continuous extracting with methanol, hexane and chloroform. The final chloroform solution was concentrated and reprecipitated in methanol to afford purified copolymers as dark purple solids. The molecular structures of the resulting

Polymer Chemistry Accepted Manuscript

copolymers were confirmed with ^{1}H NMR spectroscopy and elemental analysis. As expected, both copolymers have good solubility in chlorinated organic solvents due to the alkyl side chains attached on the polymer backbones, such as chloroform, chlorobenzene, *o*-dichlorobenzene, which would be important for fabrication of their devices by wet processes. The number-average molecular weight (M_n) and a polydispersity index (PDI) were determined by gel permeation chromatography (GPC) using $CHCl_3$ as the eluent at 80 ^oC and monodisperse polystyrene as the standard. Polymer **PDTS-ID** has a M_n of 12.8 kDa and polydispersity index (PDI) of 1.75, while **PDTS-FID** has a little higher M_n of 15.2 kDa and a larger PDI of 1.84. **PDTS-ID** and **PDTS-FID** also exhibit good thermal stabilities with decomposition temperatures over 370 ^oC (5% weight loss) under nitrogen atmosphere, investigated by thermal gravimetric analysis (TGA) (Fig. 1). The thermal properties are adequately suitable for PSC fabrications and evaluations. No phrase transition was observed for both copolymers by differential scanning calorimetry (DSC) from room temperature to 250 ^oC.

Optical properties

Fig. 2a showed the UV-vis absorption spectra of **PDTS-ID** and **PDTS-FID** in chloroform solutions and in thin solid films. The copolymers exhibit a similar feature with two main peaks both in solutions and in films, which is a common feature of D-A copolymers.[4,16] The weak absorption band within high-energy region is attributed to the localized π–π transition, and the strong band within low-energy region is related to an intramolecular charge transfer (ICT) between electron-rich donors and

Polymer Chemistry Accepted Manuscript

electron-poor acceptors.[8,13b,16b] As shown in Fig. 2a, **PDTS-ID** showed wide absorptions ranging from 300 to 800 nm with main peaks at 438 and 736 nm. Polymer **PDTS-FID** with fluorine atoms exhibited a similar shape but a red-shifted absorption with main peaks at 439 and 742 nm. This could be attributed to the more planar geometry of the molecular backbone of **PDTS-FID**, favoring the overlap between the π-orbitals along the polymeric chain and extending the conjugation length of the whole polymeric system[15] as confirmed by Density Functional Theory (DFT) calculations (reported below). As compared to their counterparts in the solution state, both copolymers show slightly broader peaks in the wavelength range of 300-850 nm (Fig. 2b). Because of the difference of interchain packing, **PDTS-ID** and **PDTS-FID** films showed different red-shifts of 3, 3 nm and 7, 3 nm, respectively. This slight red-shift phenomena can be explained by the somewhat formation of π-stacked structures even in their chloroform solutions. The introduction of fluorine atoms would facilitate the aggregation of polymer backbones through some supramolecular interactions, such as F-H, F-πF and F-S interactions.[6b,6g,15,17] The vibrational shoulder peak of a low-energy absorption band would also confirm this type of aggregation.[15,17] The optical band-gap of **PDTS-ID** and **PDTS-FID** were calculated to be 1.52 and 1.49 eV from the onset absorption edges of the corresponding UV-vis absorption in thin solid film. The obtained low band gaps of these copolymers with broad absorption bands are very important to harvest more solar photons in the fabricated PSCs later.

Electrochemical properties

Polymer Chemistry Accepted Manuscript

The appropriate energy levels are important for rational design and fabrication of high performance PSCs.[2] Cyclic voltammetry (CV) was employed to examine the electrochemical properties and evaluate the highest occupied molecular orbital (HOMO) and lowest unoccupied molecular orbital (LUMO) energy levels of the resulting copolymers. The measurements were performed in a three-electrode cell in 0.1 M tetrabutylammonium perchlorate (n-Bu_4NClO_4)-acetonitrile solution. A platinum plate coated with a thin film of the copolymer, a platinum wire and Ag/AgCl (0.1 M) were used as the work, counter and reference electrodes, respectively. The energy level of the Ag/AgCl reference electrode was calibrated against the ferrocene/ferrocenium (Fc/Fc^+) system to be 4.40 eV by using previous methods.[18] Fig. 3a displays the electrochemical properties of the thin polymer films, and the electrochemical data are summarized in Table 2. Reversible p-doping/dedoping and n-doping/dedoping processes occurred for both copolymers in the positive and negative potential ranges. The onset oxidation potentials ($E_{ox,onset}$)/reduction potentials ($E_{red,onset}$) of **PDTS-ID** and **PDTS-FID** were 1.02/-0.58 and 1.10/-0.46 eV, respectively. Thus, the HOMO/LUMO energy levels of **PDTS-ID** and **PDTS-FID** were calculated to be -5.42/-3.82 and -5.50/-3.94 eV, respectively.[2] The electrochemical band gaps (E_g) of **PDTS-ID** and **PDTS-FID** were calculated from the related energy levels to be around 1.60 and 1.56 eV, respectively. The discrepancies between the electrochemical and optical band gaps presumably resulted from the exciton binding energies of the copolymers and/or the interfacial barriers for charge injection.[19] In order to make a clear comparison, the electronic energy level diagram

Polymer Chemistry Accepted Manuscript

of the copolymers and $PC_{71}BM$ was described in Fig. 3b. The LUMO gap of 0.06-0.18 eV and the HOMO gap of 0.50-0.58 eV between the copolymers and $PC_{71}BM$ are large enough to overcome the intrachain exciton binding energy and thus guarantee efficient exciton dissociation and transfer.[20] From the CV results, polymer **PDTS-FID** processes the lower HOMO and LUMO energy levels as well smaller band gap because of the introduced fluorination effect, which is helpful to obtain higher open-circuit voltage (V_{oc}) and short circuit current density (J_{sc}) values of its PSCs.[21,3,4]

Theoretical calculations

In order to further investigate the impact of fluorine substitution on the optoelectronic properties of copolymers, theoretical calculations were also carried out to reveal the optimized molecular structures, HOMO and LUMO energy levels by using density functional theory (DFT) at the B3LYP/6-31G(d) level (Fig. 4).[4c,22] For computational simplification, long alkyl chains were replaced by methyl groups because they did not significantly affect the equilibrium geometries or electronic properties.[4c,22] The polymer backbones were also simplified to three repeating units (trimers).[4c,22] The dihedral angle between the fluorinated isoindigo unit (**FID**) and adjacent thiophene in the trimer of **PDTS-FID** (~0.01°) is similar to that in **PDTS-ID** (~20.85°). The small dihedral angle is indicative of planar conformation and effective conjugation through π orbitals.[23] The calculated HOMO and LUMO wave functions of the trimers are shown in Fig. 4a. Both polymers show similar distributions for the HOMO and LUMO. The electron density of HOMO and LUMO was mainly distributed in the

Polymer Chemistry Accepted Manuscript

middle part of the conjugated molecular skeleton, however, the HOMO and LUMO were mainly focused on the donor (**DTS**) and accepter (**ID** or **FID**) units. Compared with HOMO, HOMO-1 orbitals moved from middle part to two side parts and still mainly distributed on the accepter units, which implied that the internal charge transfers were possible in these conjugation systems. On the other hand, the similar transfer trend is observed from LUMO to LUMO+1. The HOMO and LUMO energy levels of **PDTS-ID** and **PDTS-FID** trimers were calculated to be -4.72/-2.87 eV and -4.78/-3.04 eV, respectively. The band gaps were then determined to be 1.85 and 1.74 eV. The calculation results indicated that the effect of fluorination on the energy levels and band gaps was similar to those results obtained from the CV and UV-vis evaluations. The optimized molecular geometries of the trimers of **PDTS-ID** and **PDTS-FID** are illustrated in Fig. 4b. The results indicated that they favored planar conformations both from top and side views, which could enable the electrons to be delocalized across the whole conjugated molecular system for achieving higher carrier mobility.[24] It is interesting to note that **PDTS-FID** with **FID** accepter exhibits higher planarity than **PDTS-ID**, especially from side view observations. The linear and planar polymer backbones would enhance the intermolecular π–π stacking and enable **PDTS-FID** to obtain ordered packing in the solid state.[22]

Hole and electron mobility

The effects of the fluorination on the electrical transport properties of the resulting copolymers were studied by measuring the hole and electron mobility of each of the two copolymers. It is well known that high charge mobility will enable better charge

Polymer Chemistry Accepted Manuscript

transport within an active layer in PSCs without large photocurrent loss caused by recombination of opposite charges. The enhanced carrier mobility would be expected by introduction of fluorine atoms on the skeleton of isoindigo. Thus, hole-only (ITO/PEDOT:PSS/polymer:$PC_{71}BM$(1:2)/MoO_3/Au) and electron-only devices (ITO/Al/polymer:$PC_{71}BM$(1:2)/Ca/Al) were fabricated to measure the carrier mobilities of **PDTS-ID** and **PDTS-FID** blend films *via* a space charge limit current (SCLC) method.[25] The mobility values were calculated by fitting the dark current to the model of a single carrier SCLC, which is described by the following equation:

$$J = \frac{9}{8}\varepsilon_0\varepsilon_r\mu_h\frac{V^2}{d^3}$$

where J is the current, μ_h is the zero-field mobility, ε_0 is the permittivity of free space, ε_r is the relative permittivity of the material, d is the thickness of the active layer, and V is the effective voltage. The effective voltage can be obtained by subtracting the built-in voltage (V_{bi}) and the voltage drop (V_s) from the substrate's series resistance from the applied voltage (V_{appl}), $V=V_{appl} - V_{bi} - V_s$. The hole mobility can be calculated from the slope of the $J^{1/2} \sim V$ curves. The results are plotted as $J^{1/2}$ *vs.* V, as shown in Fig. 5. According to above equation and Fig. 5, the hole and electron mobilities of **PDTS-ID** and **PDTS-FID** blend films are determined to be 2.3×10^{-3}, 3.8×10^{-3} cm^2 V^{-1} s^{-1} and 6.5×10^{-4}, 9.2×10^{-4} cm^2 V^{-1} s^{-1}, respectively. As expected, **PDTS-FID** blend film processes higher hole and electron mobility under the same conditions, which is about 1.7 and 1.4 times than those of **PDTS-ID** blend film. The increased carrier mobility of polymer **PDTS-FID** originates from the better planarity and backbone packing with **FID** accepter blocks, which has been discussed in the

Polymer Chemistry Accepted Manuscript

section of theoretical calculations.

Photovoltaic properties

To explore the photoelectric conversion properties of these two copolymers, BHJ polymer solar cells were fabricated and evaluated with the device structure of ITO/PEDOT:PSS/copolymer:$PC_{71}BM$/Ca/Al. The device-fabrication procedure is described in the experimental section. The performance of PSCs was strongly affected by the processing parameters, such as the choice of solvent, blend ratio of the copolymer and $PC_{71}BM$, and the additive effects. We fabricated and investigated the performance of a lot of devices under a variety of conditions. Optimal fabrication conditions were obtained from a *o*-dichlorobenzene (*o*-DCB) solution of a copolymer:$PC_{71}BM$ ratio of 1:2 (w/w) with 1% 1,8-diiodooctane (DIO). All the PSC devices in this work were evaluated under simulated 100 mW cm^{-2}, AM 1.5G illumination. The current density-voltage (J-V) curves are plotted in Fig. 6a. For a clear comparison, the thickness of the active layers, open-circuit voltage (V_{oc}), short-circuit current density (J_{sc}), fill factor (FF) and power conversion efficiency (PCE) of the devices are summarized in Table 3. In agreement with the positive effect of fluorination on the performance,[6b,6g,15,17] **PDTS-FID** was found to be a suitable donor material for PSC applications.

As shown in Fig. 6a, **PDTS-ID** device showed a PCE of 3.39% with V_{oc} of 0.83 V, J_{sc} of 7.62 mA cm^{-2}, and FF of 0.53. When using **PDTS-FID** as the donor material, the PSC exhibited a higher PCE of 4.29%. The superior performance was attributed the improved V_{oc}, J_{sc} as well as FF values. The fluorine substitution afforded

Polymer Chemistry Accepted Manuscript

PDTS-FID with a deeper HOMO energy level, smaller band gap as well as higher hole mobility, which is positive for increasing the V_{oc} and J_{sc} of the related PSCs. The increased J_{sc} was also confirmed by the external quantum efficiency (EQE) evaluation (Fig. 6b). The photocurrent response of all the devices covered the range of 300−850 nm. However, **PDTS-FID** showed a broader and higher curve shape. The maximum EQE plateau of **PDTS-FID** reached 39%, which is higher than that of **PDTS-ID** resulting in more efficient light harvesting and higher J_{sc} value. The J_{sc} values calculated by integrating the EQE curves with an AM 1.5G reference spectrum are within 5% error compared to the corresponding J_{sc} values obtained from the J-V curves. Moreover, the improvement in FF could be due to the formation of the optimal blend film morphology. The good phase separation of the active layer is known to be very important parameter for obtaining high efficiency of the PSCs.[3,4,6] Transmission electron microscopy (TEM) was employed here to study the morphology of the copolymer:$PC_{71}BM$ films (1:2, w/w, with 1% DIO). As shown in Fig. 7, the blend films based on **PDTS-ID** and **PDTS-FID** showed uniform and bi-continuous networks, indicating the good miscibility between the polymer donor and $PC_{71}BM$. The interpenetrating network between polymer and $PC_{71}BM$ provided a large interface area for efficient charge separation and transfer to achieve reasonable J_{sc} and FF in their PSCs. It is easy to see that both morphologies exhibited some fibril features. When the fluorine atoms were introduced, the fibril features of **PDTS-FID** blend became more evident and the length of the fiber was increased, which is also benefit to improve charge separation and transport in the photovoltaic devices.[22]

Polymer Chemistry Accepted Manuscript

The inverted device structures should have a higher performance and longer-term stability compared to conventional devices. Therefore, inverted PSCs were then fabricated and evaluated based on copolymer:$PC_{71}BM$ blends (1:2, with 1% DIO) as the active layers with the structure of ITO/ZnO/PNFBr/copolymer:$PC_{71}BM$/MoO_3/Ag. The inverted PSCs were also fabricated with the optimal conditions. ZnO and MoO_3 were chosen as electron-transport and hole-transport layers, respectively. The illuminated J-V and EQE curves of the devices are plotted in Fig. 6, and the photovoltaic data are summarized in Table 3. The inverted devices exhibited an enhanced performance with PCEs of up to 3.85 and 5.79% for **PDTS-ID** and **PDTS-FID**, respectively, which were 1.14 and 1.35 times compared to those obtained from the conventional devices. The enhancement of efficiency is mainly a result of the increased J_{sc} and FF. Especially for polymer **PDTS-FID**, the J_{sc} are increased from 9.07 to 10.77 mA cm^{-2}, and FF are increased from 0.55 to 0.64, resulting in the highest PCE of 5.79%. The increased FF might be due to the improved interfacial contact in an inverted device structure, leading to a more efficient charge collection and less electron-hole recombination.[6d] On the other hand, the improved J_{sc} could also be confirmed by the EQE results. Compared the conventional device based on **PDTS-FID**, the curve shape of the inverted device became broader and the maximum EQE increased to about 45% from 38%. The results indicated that this type of polymeric materials containing **DTS** and **FID** segments would have a promising usage in large-area polymer solar cell application. We believe the photovoltaic performance of can be further improved by the molecular design and preparation

Polymer Chemistry Accepted Manuscript

processes, such as adjusting side chains, changing bridge groups, altering molecular weight and so on.

Conclusions

Isoindigo (**ID**) and dithienosilole (**DTS**) are important building blocks for construction of efficient low band-gap photovoltaic copolymers. To investigate the effect of fluorination on the optical, electrochemical, carrier mobility and photovoltaic properties, two **DTS** copolymers (**PDTS-ID** and **PDTS-FID**) consisting of **ID** or **FID** were synthesized and characterized. The fluorination enable **PDTS-FID** with smaller band-gap, lower-lying HOMO and LUMO energy level as well as higher hole mobility, which could be attributed the more electron deficient character and more rigid planar structure of **FID** moiety. BHJ polymer solar cells were fabricated and evaluated using the resulting copolymers as donor materials. Conventional devices exhibited 3.39% and 4.29% PCE for **PDTS-ID** and **PDTS-FID**, respectively. When using an inverted device structure, the J_{sc} and FF were improved simultaneously to afford higher efficiencies. **PDTS-FID** device showed the best PCE up to 5.79%, with a V_{oc} of 0.84 V, J_{sc} of 10.77 and FF of 0.64. The results obtained in this work provide valuable information on the elaborate design of ID-based copolymers for the large-area PSC applications.

Experimental

Materials

All chemicals were purchased in reagent grade from Aladdin, Adamas. Aldrich, Alfa Aesar and Acros Chemical Co., and used without further purification. All solvents

Polymer Chemistry Accepted Manuscript

were freshly distilled immediately prior to use. The dithienosilole monomers (**DTS-Sn**) and isoindigo monomers (**ID** and **FID**) were synthesized according to our previous procedures.[15,16]

Characterization

The nuclear magnetic resonance (NMR) spectra were collected on a Bruker ARX 400 NMR spectrometer with *d*-chloroform as the solvent and tetramethylsilane (TMS) as the internal standard. Elemental analysis was performed by a Carlo Erba 116 Elemental Analyzer. Molecular weights of the copolymers were determined using Waters 1515 GPC analysis with chloroform as eluent and polystyrene as standard. Thermogravimetric analysis (TGA) was conducted on a TA Instrument Model SDT Q600 simultaneous TGA/DSC analyzer at a heating rate of 10 ^{o}C min^{-1} under a N_2 flow rate of 90 mL min^{-1}. UV-vis spectra were obtained on a Carry 300 spectrophotometer. Cyclic voltammetry (CV) measurements were made at room temperature on a CHI660 potentiostat/galvanostat electrochemical workstation at a scan rate of 50 mV s^{-1}, with a platinum wire counter electrode and an Ag/AgCl reference electrode in an anhydrous nitrogen-saturated acetonitrile solution (0.1 mol L^{-1}) of tetrabutylammonium perchlorate (Bu_4NClO_4). The redox couple of ferrocene/ferrocenium ion (Fc/Fc^+) was used as an external standard. The copolymers were coated on the platinum plate working electrodes from dilute chloroform solutions. The transmission electron microscope (TEM) investigation was performed on a JEOL EM-2100F TEM.

Device fabrication

Polymer Chemistry Accepted Manuscript

Conventional polymer solar cells (PSCs) were fabricated with ITO glass (15 Ω cm^{-2}) as an anode, Ca/Al as a cathode, and the active layer of the copolymer and $PC_{71}BM$ as a photosensitive layer. After spin-coating a 40 nm layer of PEDOT:PSS (Baytron P VP Al 4083) onto the pre-cleaned ITO substrate, the photosensitive layer was subsequently prepared by spin-coating the *o*-dichlorobenzene solution of the copolymer and $PC_{71}BM$ (w/w) on the ITO/PEDOT:PSS electrode. For the inverted devices, an about 40 nm ZnO thin film was deposited on the surface of ITO glass. The ZnO layer was pretreated with UV-ozone for 10 minutes and the conjugated polyelectrolyte of poly[(9,9-bis(3'-(N,N-dimethylamino)propyl)-2,7-fluorene)-alt-2,7-(9,9-dioctylfluorene)] dibromide (PNFBr) (5 nm) was spin-coated on the top of ZnO layer. The photoactive layer was then spin-coated on the top of above layer from *o*-dichlorobenzene solution. The photoactive layer was then thermally annealed at 110 ^{o}C for 10 minutes. Subsequently, about 10 nm MoO_3 and 100 nm Ag were deposited in turn through shadow masks by thermal evaporation.The device area was 0.09 cm^2. The current-voltage (I-V) characterization of the devices was carried out on a computer-controlled Keithley 236 Source Measurement system. The EQE was measured at a chopping frequency of 280 Hz with a lock-in amplifier (Stanford, SR830 DSP) during illumination with the monochromatic light from a xenon lamp. A solar simulator was used as the light source, and the light intensity was monitored using a standard Si solar cell. The thickness of films was measured using a Dektak 6 M surface profilometer. All of the fabrication and characterization processes were conducted in a glove box.

Polymer Chemistry Accepted Manuscript

Synthesis of the copolymers

PDTS-ID

Monomer **DTS-Sn** (0.300 g, 0.3 mmol) and monomer **ID** (0.242 g, 0.3 mmol) were dissolved in 15 mL toluene. The solution was flushed with argon for 10 min, and then Pd_2dba_3 (5.5 mg, 2 mol%) and P(*o*-tolyl)$_3$ (7.3 mg, 8%) were added into the flask. The flask was purged three times with successive vacuum and argon filling cycles. The polymerization reaction was heated to 110 ^oC and the mixture was stirred for 48 h under an argon atmosphere. 2-Tributylstannyl thiophene (23.7 mL) was added to the reaction, and then after two hours 2-bromothiophene (7.5 mL) was added. The mixture was stirred overnight to complete the end-capping reaction. The mixture was cooled to room temperature and poured slowly into 350 mL methanol. The precipitate was filtered and washed with methanol and hexane in a Soxhlet extraction apparatus to remove the oligomers and catalyst residues. Finally, the polymer was extracted with chloroform. The solution was condensed by evaporation and precipitated into methanol. The polymer **PSTS-ID** was collected as a dark purple solid with a yield of 86%. ^1H NMR ($CDCl_3$, 400 MHz, δ/ppm): 9.2-8.6 (br, 2H), 7.8-6.2 (m, 10H), 4.0-3.6 (br, 4H), 2.0-1.0 (m, 44H), 1.0-0.8 (br, 24H). Anal. Calcd for $(C_{64}H_{80}N_2O_2S_4Si)_n$: C, 72.13; H, 7.57; N, 2.63. Found: C, 71.68; H, 7.66; N, 2.72. M_n=12800; M_w=22400; PDI=1.75.

PDTS-FID

Polymer **PDTS-FID** was synthesized as dark purple solid with the yield of 83% according to the method of polymer **PDTS-ID** described above using monomer **FID**

Polymer Chemistry Accepted Manuscript

instead of compound **ID**. ^{1}H NMR ($CDCl_3$, 400 MHz, δ/ppm): 9.4-8.8 (br, 2H), 8.0-6.4 (m, 8H), 4.0-3.6 (br, 4H), 2.0-1.0 (m, 44H), 1.0-0.6 (br, 24H). Anal. Calcd for $(C_{64}H_{78}N_2O_2F_2S_4Si)_n$: C, 69.78; H, 7.14; N, 2.54. Found: C, 69.01; H, 7.22; N, 2.64. M_n=15200; M_w=28000; PDI=1.84.

Acknowledgements

This work was supported by the NSFC (20802033, 21272164), the 863 Project (No: 2013AA031901), the Youth Science and Technology Foundation of Sichuan Province (2013JQ0032), and the Fundamental Research Funds for the Central Universities (2012SCU04B01, YJ2011025).

Notes and references

1 (a) S. Günes, H. Neugebauer and N. S. Sariciftci, *Chem. Rev.,* 2007, **107**, 1324; (b) B. C. Thompson and J. M. J. Fréchet, *Angew. Chem., Int. Ed.,* 2008, **47**, 58; (c) Y. J. Cheng, S. H. Yang and C. S. Hsu, *Chem. Rev.,* 2009, **109**, 5868; (d) G. Li, R. Zhu and Y. Yang, *Nat. Photonics,* 2012, **6**, 153.

2 (a) Y. F. Li and Y. P. Zou, *Adv. Mater.,* 2008, **20**, 2952; (b) J. W. Chen and Y. Cao, *Acc. Chem. Res.,* 2009, **42**, 1709; (c) L. Y. Bian, E. W. Zhu, J. Tang, W. H. Tang and F. J. Zhang, *Prog. Polym. Sci.,* 2012, **37**, 1292.

3 (a) J. Roncali, *Chem. Rev.,* 1997, **97**, 173; (b) R. C. Coffin, J. Peet, J. Rogers and G. C. Bazan, *Nat. Chem.,* 2009, **1**, 657; (c) H. Y. Chen, J. H. Hou, A. E. Hayden, H. Yang, K. N. Houk and Y. Yang, *Adv. Mater.,* 2010, **22**, 371; (d) Q. Peng, X. J. Liu, Y. C. Qin, M. J. Li, J. Xu, G. W. Fu and L. M. Dai, *J. Mater. Chem.,* 2011, **21**, 7714; (e) X. H. Zhou, L. Q. Yang and W. You, *Macromolecules,* 2012, **45**, 607.

Polymer Chemistry Accepted Manuscript

4 (a) E. Perzon, F. Zhang, M. Andersson, W. Mammo, O. Inganäs and M. R. Andersson, *Adv. Mater.,* 2007, **19**, 3308; (b) J. H. Tsai, W. Y. Lee, W. C. Chen, C. Y. Yu, G. W. Hwang and C. Ting, *Chem. Mater.,* 2010, **22**, 3290; (c) Q. Peng, S. L. Lim, I. H. Wong, J. Xu and Z. K. Chen, *Chem.-Eur. J.,* 2012, **18**, 12140; (d) C. M. Amb, S. Chen, K. R. Graham, J. Subbiah, C. E. Small, F. So and J. R. Reynolds, *J. Am. Chem. Soc.,* 2011, **133**, 10062; (e) T. Y. Chu, J. Lu, S. Beaupré, Y. Zhang, J.-R. Pouliot, S. Wakim, J. Zhou, M. Leclerc, Z. Li, J. Ding and Y. Tao, *J. Am. Chem. Soc.,* 2011, **133**, 4250; (f) S. C. Price, A. C. Stuart, L. Yang, H. Zhou and W. You, *J. Am. Chem. Soc.,* 2011, **133**, 4625.

5 (a) Y. Liang, Z. Xu, J. Xia, S. T. Tsai, Y. Wu, G. Li, C. Ray and L. Yu, *Adv. Mater.,* 2010, **22**, E135; (b) Q. Peng, X. J. Liu, D. Su, G. W. Fu, J. Xu and L. M. Dai, *Adv. Mater.,* 2011, **23**, 4554; (c) Z. He, C. Zhong, X. Huang, W. Y. Wong, H. Wu, L. Chen, S. Su and Y. Cao, *Adv. Mater.,* 2011, **23**, 4636;

6 (a) C. E. Small, S. Chen, J. Subbiah, C. M. Amb, S. W. Tsang, T. H. Lai, J. R. Reynolds and F. So, *Nat. Photonics,* 2012, **6**, 115; (b) X. H. Li, W. C. H. Choy, L. J. Huo, F. X. Xie, W. E. I. Sha, B. F. Ding, X. Guo, Y. F. Li, J. H. Hou, J. B. You and Y. Yang, *Adv. Mater.,* 2012, **24**, 3046; (c) J. B. You, L. T. Dou, K. Yoshimura, T. Kato, K. Ohya, T. Moriarty, K. Emery, C. C. Chen, J. Gao, G. Li and Y. Yang, *Nat. Commun.,* 2013, **4**, 1446; (d) K. Li, Z. J. Li, K. Feng, X. P. Xu, L. Y. Wang and Q. Peng, *J. Am. Chem. Soc.,* 2013, **135**, 13549.

7 J. Mei, K. R. Graham, R. Stalder and J. R. Reynolds, *Org. Lett.,* **2010**, *12*, 660.

8 R. Stalder, J. Mei and J. Reynolds, *Macromolecules,* **2010**, *43*, 8348.

Polymer Chemistry Accepted Manuscript

9 G. Zhang, Y. Fu, Z. Xie and Q. Zhang, *Macromolecules,* **2011**, *44*, 1414.

10 B. Liu, Y. Zou, B. Peng, B. Zhao, K. Huang, Y. He and C. Pan, *Polym. Chem.,* 2011, **2**, 1156.

11 E. G. Wang, Z. F. Ma, Z. Zhang, P. Henriksson, O. Inganäs, F. L. Zhang and M. R Andersson, *Chem. Commun.,* 201**1**, **47**, 4908

12 E. Wang, Z. Ma, Z. Zhang, K. Vandewal, P. Henriksson, O. Inganäs, F. Zhang and M. R. Andersson, *J. Am. Chem. Soc.,* 2011, **133**, 14244.

13 (a) R. Stalder, C. Grand, J. Subbiah, F. So and J. R. Reynolds, *Polym. Chem.,* 2012, **3**, 89; (b) Z. Ma, E. Wang, M. E. Jarvid, P. Henriksson, O. Inganäs, F. Zhang and M. R. Andersson, *J. Mater. Chem.,* 2012, **22**, 2306; (c) C. Hu, Y. Y. Fu, S. G. Li, Z. Y. Xie and Q. Zhang, *Polym. Chem.,* 2012, **3**, 2949; (d) Y. Koizumi, M. Ide, A. Saeki, C. Vijayakumar, B. Balan, M. Kawamotoa, S. Seki, *Polym. Chem.,* 2013, **4**, 484; (e) K. Mahmood, Z. P. Liu, C. H. Li, Z. Lu, T. Fang, X. Liu, J. J. Zhou, T. Lei, J. Pei and Z. S. Bo, *Polym. Chem.,* 2013, **4**, 3563; (f) P. Sonar, H. S. Tan, S. Y. Sun, Y. M. Lam and A. Dodabalapur, *Polym. Chem.,* 2013, **4**, 1983.

14 T. Lei, J. H. Dou, Z. J. Ma, C. H. Yao, C. J. Liu, J. Y. Wang and J. Pei, *J. Am. Chem. Soc.,* 2012, **134**, 20025.

15 Y. C. Yang, R. M. Wu, X. Wang, X. P. Xu, Z. J. Li, K. Li and Q. Peng, *Chem. Commun.,* 2014, **50**, 439.

16 (a) Z. J. Li, D. Zhou, L. X. Li, Y. Li, Y. J. He, J. Liu and Q. Peng, *Polym. Chem.,* 2013, **4**, 2496; (b) Z. G. Zhang, Y. L. Liu, Y. Yang, K. Y. Hou, B. Peng, G. J.

Polymer Chemistry Accepted Manuscript

Zhao, M. j. Zhang, X. Guo, E. T. Kang, Y. F. Li, *Macromolecules,* 2010, **43**, 9376.

17 (a) Y. Wang, S. R. Parkin, J. Gierschner and M. D. Watson, *Org. Lett.,* 2008, **10**, 3307; (b) H. Zhou, L. Yang, A. C. Stuart, S. C. Price, S. Liu and W. You, *Angew. Chem. Int. Ed.,* 2011, **50**, 2995; (c) Y. Zhang, J. Zou, C. C. Cheuh, H. L. Yip and A. K. Y. Jen, *Macromolecules,* 2012, **45**, 5427; (d) K. Feng, X. Y. Shen, Y. Li, Y. J. He, D. Huang and Q. Peng, *Polym. Chem.,* 2013, **4**, 5701; (e) J. Min, Z. G. Zhang, S. Y. Zhang, Y. F. Li, *Chem. Mater.,* 2012, **24**, 3247.

18 (a) Y. F. Li, Y. Cao, J. Gao, D. L. Wang, G. Yu and A. J. Heeger, *Synth. Met.,* 1999, **99**, 243; (b) Q. Peng, Z. Y. Lu, Y. Huang, M. G. Xie, S. H. Han, J. B. Peng and Y. Cao, *Macromolecules,* 2004, **37**, 260; (c) Q. Peng, J. B. Peng, E. T. Kang, K. G. Neoh and Y. Cao, *Macromolecules,* 2005, **38**, 7292.

19 P. T. Wu, F. S. Kim, R. D. Champion and S. A. Jenekhe, *Macromolecules,* 2008, **41**, 7021.

20 C. J. Brabec, C. Winder, N. S. Sariciftci, J. C. Hummelen, A. Dhanabalan, P. A. van Hal and R. A. J. Janssen, *Adv. Funct. Mater.,* 2002, **12**, 709.

21 (a) M. C. Scharber, D. Mühlbacher, M. Koppe, P. Denk, C. Waldauf, J. Heeger and C. J. Brabec, *Adv. Mater.,* 2006, **18**, 789; (b) B. C. Thompson, Y. G. Kim, T. D. McCarley and J. R. Reynolds, *J. Am. Chem. Soc.,* 2006, **128**, 12714.

22 Z. Zeng, Y. Li, J. F. Deng, Q. Huang and Q. Peng, *J. Mater. Chem. A,* 2014, 2, 653.

23 J. Kim, Y. S. Kwon, W. S. Shin, S. J. Moon and T. Park, *Macromolecules* 2011,

Polymer Chemistry Accepted Manuscript

44, 1909.

24 S. Cho, J. H. Seo, S. H. Kim, S. Song, Y. Jin, K. Lee, H. Suh and A. J. Heeger, *Appl. Phys. Lett.,* 2008, **93**, 263301.

25 V. Shrotriya, Y. Yao, G. Li and Y. Yang, *Appl. Phys. Lett.,* 2006, **89**, 063505.

26 Q. Peng, Q. Huang, X. B. Hou, P. P. Chang, J. Xu and S. J. Deng, *Chem. Commun.,* 2012, **48**, 11452.

Polymer Chemistry Accepted Manuscript

Legends for Schemes, Figures and Tables

Scheme 1. Synthetic route to PDTS-ID and PDTS-FID.

Fig. 1. TGA curves of PDTS-ID and PDTS-FID with a heating rate of 10 ^{o}C min^{-1}

Fig. 2. Normalized UV-vis absorption spectra of copolymers in dilute chloroform solutions (a) and thin-films cast from chloroform solutions (b).

Fig. 3. (a) Cyclic voltammograms of thin films of copolymers in 0.1 M *n*-Bu_4NClO_4 solution in acetonitrile at a scan rate of 0.05 V s^{-1}. (b) HOMO and LUMO energy levels of copolymers and $PC_{71}BM$.

Fig. 4. Optimized molecular orbital surfaces of the LUMO+1, LUMO, HOMO and HOMO-1 for the model trimer of PDTS-ID (left) and PDTS-FID (right), obtained by Gaussian 09 at the B3LYP/6-31G(d) level. (b) Optimized molecular structures for the model trimers of PDTS-ID (left) and PDTS-FID (right) with top and side views.

Fig. 5. $J^{1/2}$-V characteristics of copolymer-based hole-only and electron-only devices measured at ambient temperature.

Fig. 6. (a) J-V curves of polymer solar cells based on copolymers together with $PC_{71}BM$ under AM 1.5 illumination. (b) EQE curves of polymer solar cells based on copolymers together with $PC_{71}BM$.

Fig. 7. TEM images of PTDTS-ID/$PC_{71}BM$ (a) and PDTS-FID/$PC_{71}BM$ (b). Scale bar=100 nm.

Table1 Molecular weights and thermal properties of the copolymers

Polymer Chemistry Accepted Manuscript

Table 2 Optical and electrochemical data of the copolymers

Table 3 Performance of polymer solar cells tested under AM 1.5 simulated illumination.

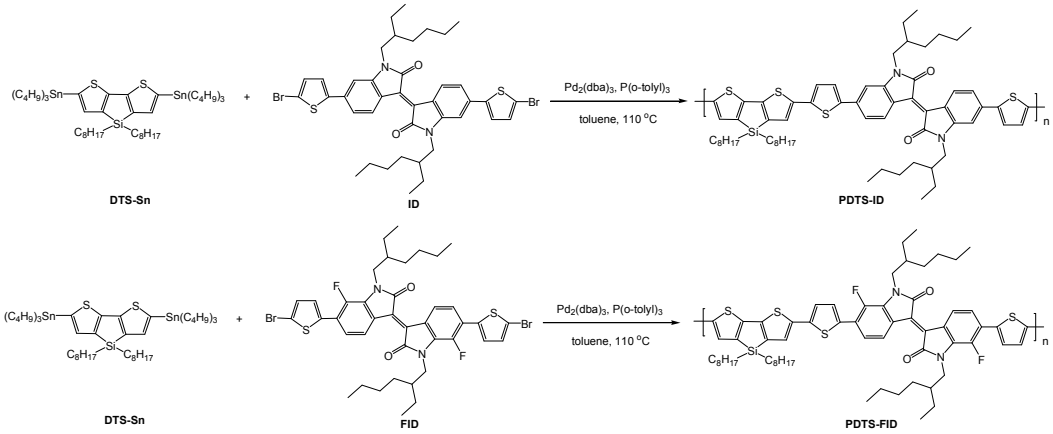

Scheme 1. Synthetic route to PDTS-ID and PDTS-FID.

Polymer Chemistry Accepted Manuscript

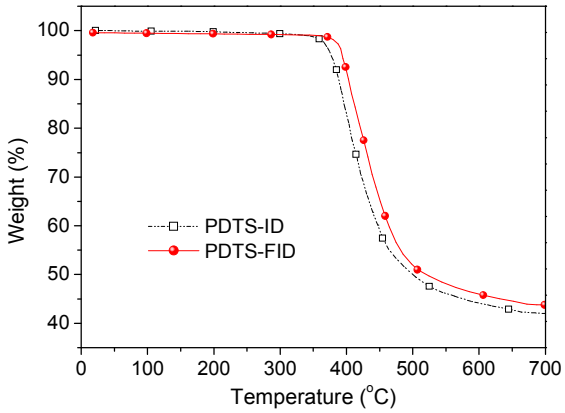

Fig. 1 TGA curves of PDTS-ID and PDTS-FID with a heating rate of 10 ^{o}C min^{-1}.

Polymer Chemistry Accepted Manuscript

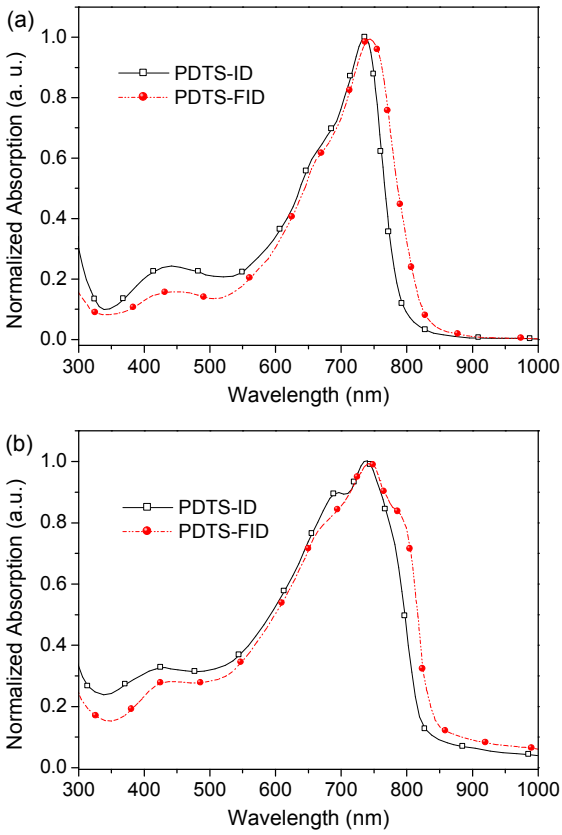

Fig. 2 Normalized UV-vis absorption spectra of copolymers in dilute chloroform solutions (a) and thin-films cast from chloroform solutions (b).

Polymer Chemistry Accepted Manuscript

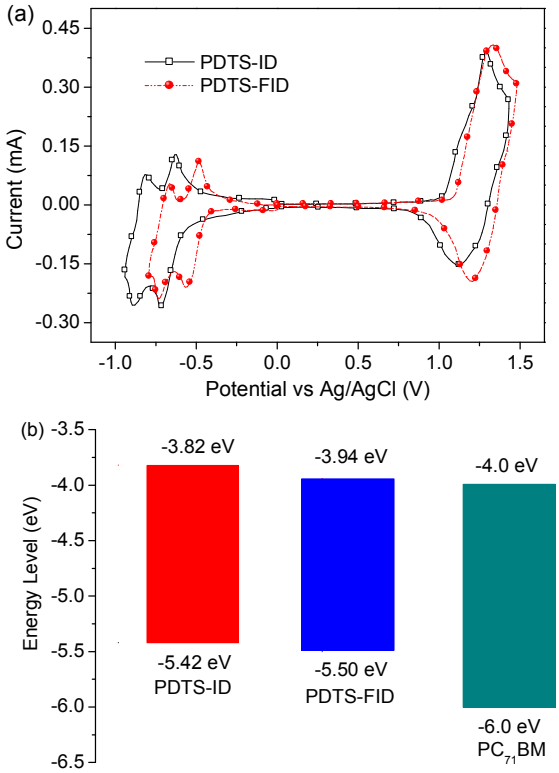

Fig. 3 (a) Cyclic voltammograms of thin films of copolymers in 0.1 M *n*-Bu_4NClO_4 solution in acetonitrile at a scan rate of 0.05 V s^{-1}. (b) HOMO and LUMO energy levels of copolymers and $PC_{71}BM$.

Polymer Chemistry Accepted Manuscript

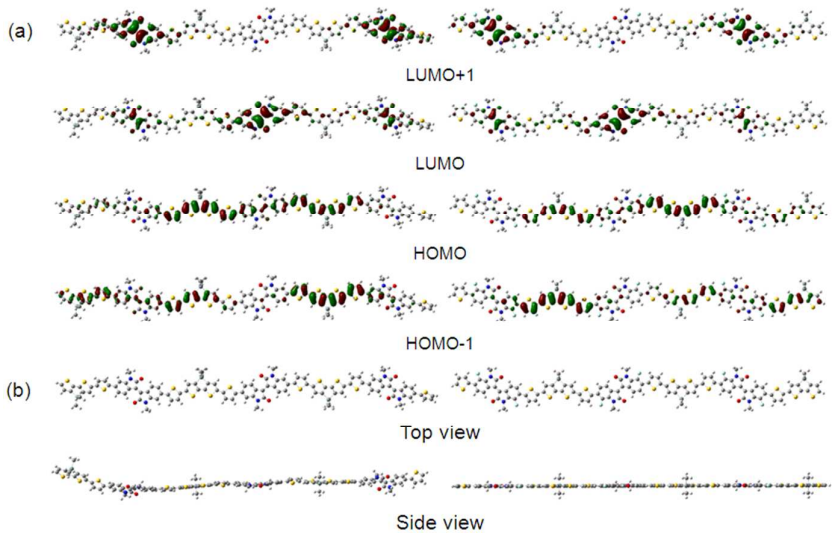

Fig. 4 Optimized molecular orbital surfaces of the LUMO+1, LUMO, HOMO and HOMO-1 for the model trimer of PDTS-ID (left) and PDTS-FID (right), obtained by Gaussian 09 at the B3LYP/6-31G(d) level. (b) Optimized molecular structures for the model trimers of PDTS-ID (left) and PDTS-FID (right) with top and side views.

Polymer Chemistry Accepted Manuscript

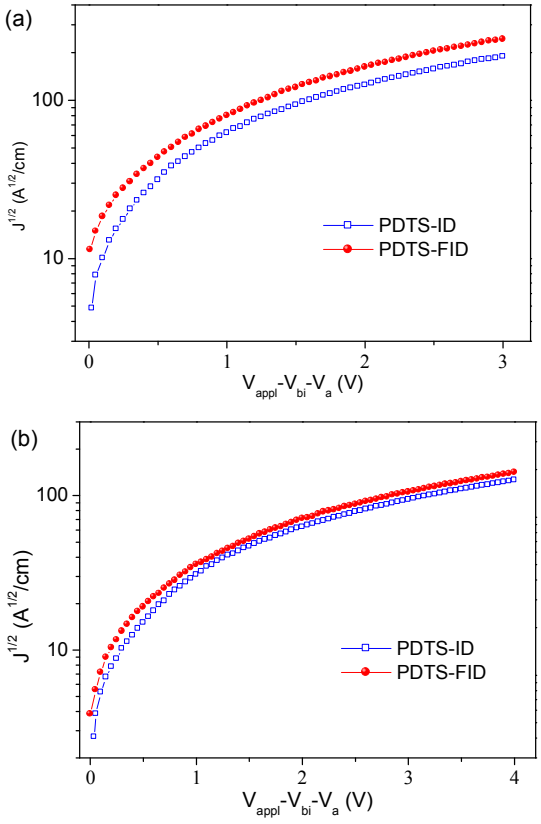

Fig. 5 $J^{1/2}$–V characteristics of copolymer-based hole-only (a) and electron-only (b) devices measured at ambient temperature.

Polymer Chemistry Accepted Manuscript

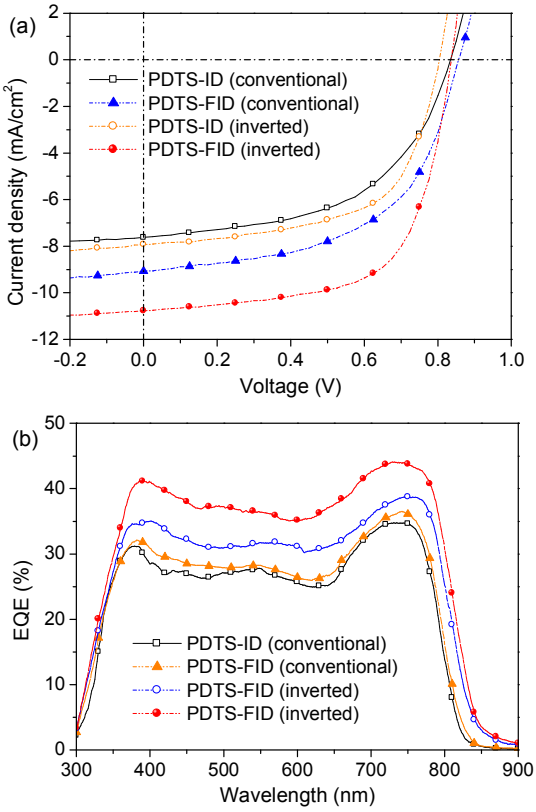

Fig. 6 (a) J–V curves of polymer solar cells based on copolymers together with $PC_{71}BM$ under AM 1.5 illumination. (b) EQE curves of polymer solar cells based on copolymers together with $PC_{71}BM$.

Polymer Chemistry Accepted Manuscript

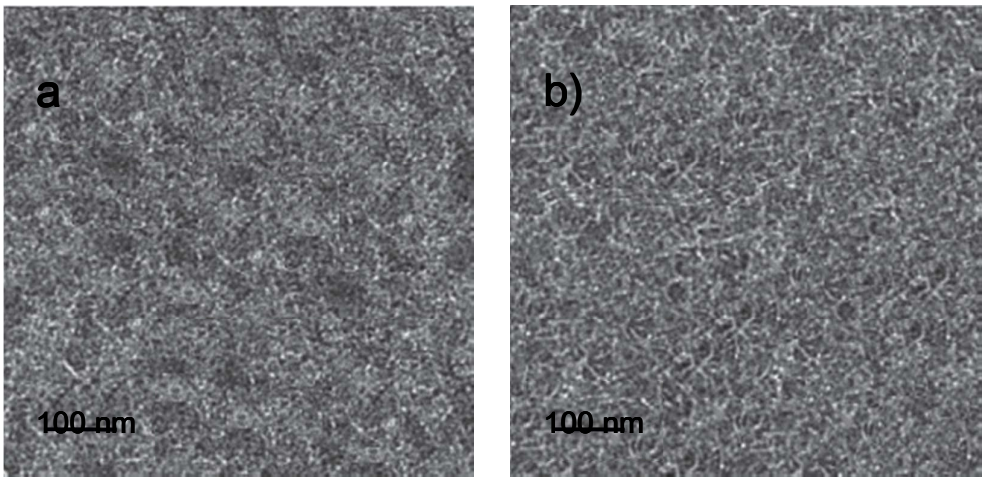

Fig. 7 TEM images of PTDTS-ID/$PC_{71}BM$ (a) and PDTS-FID/$PC_{71}BM$ (b). Scale bar = 100 nm.

Polymer Chemistry Accepted Manuscript

Table1 Molecular weights and thermal properties of the copolymers

polymers	Yield (%)	M_w[a](kDa)	M_n[a](kDa)	PDI[a]	T_d (°C)[b]
PDTS-ID	86	22.4	12.8	1.75	375
PDTS-FID	90	28.0	15.2	1.84	394

[a]Molecular weights and polydispersity indices were determined by GPC in chloroform using polystyrene as standards. [b]Onset decomposition temperature measured by TGA under N_2.

Polymer Chemistry Accepted Manuscript

Table 2 Optical and electrochemical data of the copolymers

polymers	Abs. (nm) λ_{max}^{Sol}	Abs. (nm) λ_{max}^{film}	E_g^a (eV)	HOMO (eV)	LUMO (eV)	E_g^b (eV)
PDTS-ID	438, 736	441,739	1.52	-5.42	-3.82	1.60
PDTS-FID	439, 742	446,745	1.49	-5.50	-3.94	1.56

[a]Optical band gap was estimated from the wavelength of the optical absorption edge of the copolymer film.

[b]Electrochemical band gap was calculated from the LUMO and HOMO energy levels.

Polymer Chemistry Accepted Manuscript

Table 3 Performance of polymer solar cells tested under AM 1.5 simulated illumination.

polymers	thickness (nm)	V_{oc} (V)	J_{sc} (mA cm^{-2})	FF	PCE (%)
PDTS-ID[a]	110	0.83	7.62	0.53	3.39
PDTS-ID[b]	105	0.81	7.92	0.60	3.85
PDTS-FID[a]	100	0.86	9.07	0.55	4.29
PDTS-FID[b]	95	0.84	10.77	0.64	5.79

[a]Measured from the conventional devices. [b]Measured from the inverted devices.

Polymer Chemistry Accepted Manuscript

The table of contents entry

Low bandgap copolymers derived from fluorinated isoindigo and dithienosilole: synthesis, properties and photovoltaic applications

Zhenguo Wang, Jie Zhao, Ying Li, and Qiang Peng

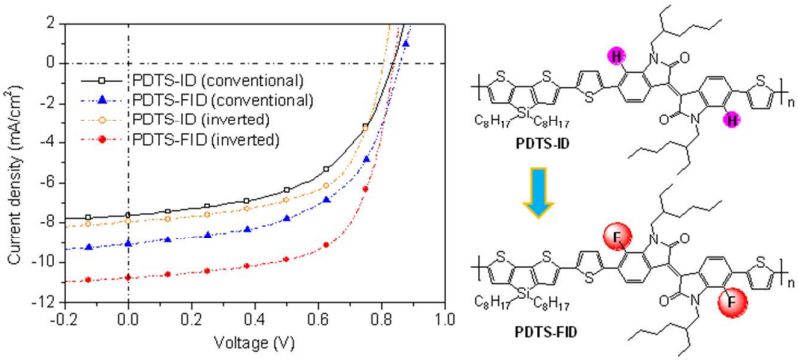

Fluorination of isoindigo affords dithienosilole-based low band-gap copolymer with low-lying energy levels, strong and broad absorption, high carrier mobility as well as efficient power conversion efficiency.

Polymer Chemistry Accepted Manuscript